

# Unfolding Properties of Recombinant Human Serum Albumin Products Are Due To Bioprocessing Steps

Brian E. Lang and Kenneth D. Cole

National Inst. of Standards and Technology, Biosystems and Biomaterials Div., Gaithersburg, MD 20899

DOI 10.1002/btpr.1996

Published online 00 Month 2014 in Wiley Online Library (wileyonlinelibrary.com)

We have used differential scanning calorimetry (DSC) to determine the unfolding properties of commercial products of human serum albumin (HSA) prepared from pooled human blood, transgenic yeast, and transgenic rice. The initial melting temperatures ( $T_{mI}$ ) for the unfolding transitions of the HSA products varied from 62°C to 75°C. We characterized the samples for purity, fatty acid content, and molecular weight. The effects of adding fatty acids, heat pasteurization, and a low pH defatting technique on the transition temperatures were measured. Defatted HSA has a structure with the lowest stability ( $T_m$  of ~62°C). When fatty acids are bound to HSA, the structure is stabilized ( $T_m$  of ~64–72°C), and prolonged heating (pasteurization at 60°C) results in a heat-stabilized structural form containing fatty acids ( $T_m$  of ~75–80°C). This process was shown to be reversible by a low pH defatting step. This study shows that the fatty acid composition and bioprocessing history of the HSA commercial products results in the large differences in the thermal stability. © 2014 American Institute of Chemical Engineers *Biotechnol. Prog.*, 000:000–000, 2014

**Keywords:** human serum albumin, differential scanning calorimetry (DSC), recombinant proteins, biopharmaceutical, thermal unfolding, and thermodynamics

## Introduction

The serum albumins have a central role in maintaining osmotic balance in blood and transporting physiologically important ligands (fatty acids, hormones, and drugs).<sup>1</sup> Human serum albumin (HSA) is used to extend blood volume, as a growth promoter in cell culture, and in drug formulations for effective delivery.<sup>2</sup> HSA in drug formulations can function to effectively reduce oxidation, aggregation, and non-specific absorption of protein pharmaceuticals.<sup>3</sup> Because of these important pharmaceutical applications, HSA is produced in large quantities from human donor plasma. However, there has been much interest in the production of HSA using recombinant DNA technology in order to reduce the risk of blood-borne pathogens and to lower cost. Commercial HSA products are currently available from transgenic rice and yeast.<sup>4</sup> The HSA produced at high concentrations in rice (*Oryza sativa*) grains was shown to have the same amino acid sequence and to be biologically equivalent (cell culture growth stimulation and treating liver damage due to cirrhosis) to the human-derived product.<sup>5</sup> Yeast (*Pichia pastoris* or *Saccharomyces cerevisiae*) are also used to produce HSA in large quantities with the correct amino acid sequence and similar biological properties.<sup>6,7</sup> Recombinant HSA has been used in cell culture media for Chinese hamster ovary cell to avoid the use of serum products, resulting in a chemically defined media.<sup>8</sup> It is important to ensure that the commercial products have the same biological

and physical properties when compared to the natural product, in this case HSA, produced from human donors.

Thermal stability measurements provide information on protein unfolding, aggregation, and the reversibility of the unfolding process after being heated above ambient temperature. The thermal unfolding process can be readily monitored by differential scanning calorimetry (DSC) that can reliably determine the melting temperature, and can also be used for the determination of other thermodynamic parameters, such as the calorimetric and van't Hoff enthalpies,  $\Delta H_d$  and  $\Delta H_{vH}$ , respectively. DSC can also be used to accurately determine the purity of proteins based on differences in the unfolding properties.<sup>9</sup>

Like many proteins, the thermal unfolding properties of HSA are affected by pH, ionic strength, protein concentration, and the temperature scan rate, often making it difficult to compare one study to another. However, albumin samples run under the same conditions should have very similar thermal unfolding properties, provided they have the same 3-dimensional structure and bound ligands. Further complicating the thermal unfolding of the albumins is the effect of fatty acids on the relative stability of the protein. Since one of the roles of albumin is the transport of fatty acids through the body, naturally occurring albumin has bound long-chain fatty acids (typically 14–18 carbons).<sup>10,11</sup> There are seven fatty acid binding sites in HSA with different affinities.<sup>12</sup> Commercial preparations of HSA and bovine serum albumin (BSA) are often defatted or have octanoic acid or *N*-acetyl-L-tryptophan added to the formulations to increase the shelf life of the product and to decrease the rate of dimerization.

In a review of the current literature, we have found that even when keeping the variables such as pH, scan rate, and

Correspondence concerning this article should be addressed to K. D. Cole at kenneth.cole@nist.gov

**Table 1. Current Literature Values of HSA Thermal Unfolding Temperature and Unfolding Enthalpies**

Reference	pH	$T_{m1}$ (°C)	$\Delta H$ (kJ/mol)	Scan Rate (°C/min)	Bound Fatty Acids
Pico (1997) <sup>15</sup>	7.4	63.2	372	1.0	No
Celej et al. (2006) <sup>13</sup>	7.2	60.1	481	1.0	No
Rezaei-Tavirani et al. (2006) <sup>16</sup>	7.0	45.0	—	1.0	Yes
Farruggia et al. (2001) <sup>18</sup>	7.4	56.1	413	1.0	No
Watanabe et al. (2001) <sup>6</sup>	7.4	79.5	1132	1.0	Yes
Watanabe et al. (2001) <sup>6</sup>	7.4	59.7	630	1.0	No
Shrake et al. (2006) <sup>17</sup>	7.0	64.7	981	0.198	No
Shrake et al. (1984) <sup>22</sup>	7.0	66.8	—	0.237	Yes
Michnik et al. (2006) <sup>14</sup>	6.0	73.4	761	1.0	Yes
Michnik et al. (2006) <sup>14</sup>	6.0	62.5	760	1.0	No
Garidel et al. (2009) <sup>21</sup>	6.0	74.5	—	1.0	Yes
Garidel et al. (2009) <sup>21</sup>	6.0	69.3	1025	1.0	No

the presence or absence of fatty acids constant, there is considerable variation in the reported melting temperatures  $T_m$  and enthalpy values of HSA (Table 1).<sup>6,13–21</sup>

One of the biggest challenges in using protein pharmaceuticals is that there are many points along the manufacturing chain that may cause changes in the final product. The expression and processing steps may result in potential changes to the secondary and tertiary structures of the protein products. In this study, we have focused on measurement of the stability of the HSA commercial products using DSC and the effect of added fatty acids and a pasteurization bioprocessing step (heat treatment) on the stability of the products.

## Materials and Methods

### Samples

The recombinant forms of HSA was obtained from: Albumin Biosciences (lots N0311D1UCM and N121361UCM), Cyagen (lot 111027c01), Genlantis/ABS Bioscience, Invitro (DX-LR lot P0275), Kerry/Sheffield (lot 13200177773), Novazymes (lot RF010), and from Sigma Aldrich (Invitro Cellastim lots 120M1687 and 058K1478, and one undisclosed manufacturer product A0237, lot 031M1353V). HSA from pooled serum was obtained from Gemini Bioscience (West Sacramento, CA, Lot 20101008), Golden West Biologicals (Temecula, CA, lot G011501098), Octapharma Plasma (Charlotte, NC, lot C212B6671), ProSpec-Tany TechnoGene (East Brunswick, NJ, lot 1207HSA01), and Sigma-Aldrich (St. Louis, MO, lot 21K7601). NIST Standard Reference Material® (SRM) 927d BSA was used as well\*.

The samples have all been given letter designations (Table 2). Letter designations I, J, M, N, and O were obtained from pooled human blood. Several samples, E, G, and I were also defatted after being received from the manufacturer. The samples run “as is” are labeled E-1, G-1, and I-1, and those samples that were partially defatted (described in methods section) are labeled E-2, G-2, and I-2. All of the samples were exchanged into the same sodium phosphate buffer (described in the next section) to remove any preservatives and ensure a uniform ionic solution.

### SDS-PAGE

The overall purity of the samples was assessed by sodium dodecyl sulfate polyacrylamide gel electrophoresis (SDS-PAGE) using reducing conditions. The SDS-PAGE was run on a 4%–12% Bis-Tris gel with a 2-(N-morpholino) ethane-sulfonic acid buffer and stained with Coomassie Brilliant Blue G-250 (Life Technologies, Carlsbad, CA). Purity of the HSA band was determined by image analysis (Gel Pro, Media Cybernetics, Rockville, MD).

### Size exclusion chromatography and protein concentration

Size exclusion chromatography (SEC) was done using a 0.1 M sodium phosphate buffer (0.05 M sodium dibasic phosphate and 0.05 M sodium monobasic phosphate, 0.025% sodium azide, pH 6.8) at a flow rate of 0.7 mL/min with a 300 mm by 7.8 mm diameter column (Yarra 3  $\mu$ m SEC 3000, Phenomenex, Torrance, CA) monitored at 220 nm. The concentration of the HSA samples was determined using the SEC chromatography peak areas and BCA (Biuret) method for measuring protein concentration (Pierce Biotechnology, Rockford, IL). BSA was used as a calibrant.

### Fatty acid measurements

The fatty acid content of the samples was determined using a fatty acid assay kit (Biovision Incorporated, Milpitas, CA) using a colorimetric/fluorescent probe to determine the molar concentrations of the fatty acids. Calibration solutions (palmitic acid) along with the protein solutions at various concentrations were loaded onto a 96-well plate using the kit protocol, and the fluorescence measurements were made on a Biotek Synergy MX plate reader.

### Sample preparation, defatting, and DSC measurements

The albumin samples for DSC measurements were buffer exchanged into 10 mM<sup>†</sup> sodium phosphate that contained 137 mM sodium chloride and adjusted to pH = 7.40 with sodium hydroxide (phosphate buffered saline (PBS buffer)). Buffer exchange of the albumin samples was done using a NAP-5 Sephadex G-25 prep column (GE Healthcare, Pittsburgh, PA) to have a constant ionic environment and remove the small molecules associated in the albumin preparations. The partial defatting of the HSA was achieved by using a Sep-Pak C18 (500 mg) solid phase extraction column (Waters, Milford, MA). First, the pH of the albumin solution

\*Certain commercial equipment, instruments, or materials are identified in this paper in order to specify the experimental procedure adequately. Such identification is not intended to imply recommendation or endorsement by the National Institute of Standards and Technology, nor is it intended to imply that the materials or equipment identified are necessarily the best available for the purpose.

<sup>†</sup>We have used the symbol M to represent the SI units of mol/L to meet the style of the journal.

**Table 2. Analysis of the Samples Used in this Study**

Sample	Gel Purity (%)	Monomer Content (%)	Mass (kDa)	Fatty Acid Content (mole fraction)
HSA A (rice)	60	79.7	65.95	0.06
HSA B (rice)	44	85.9	66.67	2.4
HSA C (rice)	53	89.2	65.81	2.7
HSA D (yeast)	95	98.4	66.63	0.2
HSA E-1 (yeast)	95	97.3	66.58	0.5
HSA E-2			66.58	0.2
HSA F (rice)	85	94.6	66.41	0.6
HSA G-1 (yeast)	95	99.4	66.49	0.12
HSA G-2			66.49	>0.01
HSA H (rice)	49	95.0	66.03	0.01
HSA I-1 (human)	93	99.5	66.62	0.24
HSA I-2			66.62	0.11
HSA J (human)	95	95.6	66.47	2.4
HSA K (rice)	65	91.0	66.87	1.4
HSA L (rice)	81	87.0	66.55	1.6
HSA M (human)	85	86.7	66.45	2.4
HSA N (human)	95	97.7	66.51	4.4
HSA O (human)	86	92.7	66.52	3.6

Shown are the protein purity determined by gel electrophoresis (avg. normalized S.D. 6%), percentage of monomeric albumin by SEC of monomer peak (avg. normalized S.D. 1%), mass determined by MALDI-TOF (uncertainty of 0.35 kDa), and the mole fraction of fatty acid content of the proteins (avg. normalized S.D. 15%). Transgenic species are rice (*Oryza sativa*) and yeast (*Pichia pastoris* and *Saccharomyces cerevisiae*).

was adjusted to pH = 4.0 with 10 mM sodium acetate buffer pH = 3.0.<sup>23</sup> Then, the Sep-Pac column was wetted with 1 mL of methanol and then equilibrated using 10 mM phosphate, 10 mM acetate buffer, pH = 4.0. The albumin solution was added to the column and an equivalent volume of the phosphate acetate buffer was passed through the column. The eluent was collected and then returned to the PBS phosphate buffer (pH 7.4).

Additional purification was needed for sample J (Cohn fraction V from pooled). The sample was first purified by SEC using a 50 cm Sephacryl S-300 resin (60 cm × 1.5 cm column, GE healthcare, Pittsburgh, PA) using a pH = 7 phosphate buffer at a flow rate of 0.6 mL per minute. The purified fractions containing the HSA were pooled and then placed on a DEAE Sepharose column (10 cm × 1cm), and the various impurities were eluted off using a stepwise pH gradient from pH = 5.5 to pH = 4.5 acetate buffers at a flow rate of 0.5 mL per minute.<sup>24,25</sup>

Calorimetric measurements were made using a Microcal VP-DSC (GE Healthcare Biosciences, Pittsburgh, PA) using scans from 25°C to 95°C, at a scan rate of 0.0166 K/s (1 K/min) unless otherwise noted. Measurements using the DSC consisted of either 2 or 3 measurements of buffer vs. buffer to generate a baseline reference curve for the DSC at a given scan rate. The scans were followed by replicate measurements of the sample. Additionally, final measurement of the denatured protein was made in order to obtain the heat capacity of the protein without the higher order structural transitions. This was often useful in determining the nature of the baseline when fitting the transitions.

### CD measurements

Circular dichroism (CD) measurements were made with an Applied Photonics Chirascan using a quartz cuvette with a 1-mm path length at ambient temperature. Albumin solutions were made in (10 mM sodium phosphate with 50 mM sodium sulfate) buffer at pH = 7.00 with a nominal albumin

concentration of 2.6 μM. The addition of 50 mM sodium sulfate was used to keep the ionic strength the same as the buffer used for DSC. The slight difference in pH is not expected to cause significant structural changes.<sup>26</sup> The CD measurements were made from 184 nm to 300 nm with a 1 nm resolution, with a total of 10 scans for each solution that were then averaged for the final reported spectra.

### Heat treatment

The effects of heat pasteurization on the secondary structure of HSA were studied by simulating a processing step in an industrial process. Aliquots of the albumins were portioned into vials along with *cis* 9-octadecenoic acid (oleic acid) solution in PBS, giving solutions of albumin with 0, 1, and 2 mole fraction of fatty acid. The samples were then placed in a temperature controlled bath at 60°C for 12–14 h. The pasteurized samples were stored at 4°C until the thermal unfolding was measured.

### MALDI-TOF mass Spectroscopy

Molecular weights of the different albumin preparations were determined using a Voyager-DE Matrix-Assisted Laser Desorption/Ionization–Time of Flight (MALDI-TOF) mass spectrometry system from Perceptive Biosystems. Albumin samples were taken out of the phosphate buffer and placed into deionized water through buffer exchange using an Amicon Ultra 0.5 mL 30K MWCO centrifugal filter. The solutions were spun down to less than 50 μL and rinsed four times with the deionized water to remove the phosphate buffer. Protein solutions were spotted onto the MALDI plate, with 3,5-dimethoxy-4-hydroxycinnamic acid (sinapinic acid), as a solution of 20 mg/mL sinapinic acid in ACN:water:TFA (50:50:0.1) as the matrix medium. NIST SRM 927d (BSA) was used as the molecular weight calibration standard since it has a mass close to HSA. To test for reproducibility and variance in MALDI, several of the HSA samples (both recombinant and pooled HSA) and SRM 927d, were placed at six various locations on the MALDI plate. The replicate measurements of the SRM gave a standard deviation of 23 mass units, and the HSA samples have a standard deviation between 24 and 75 mass units. The remainder of the uncertainty estimate was based on bias associated with the measurement of SRM 927d.

## Results and Discussion

### Characterization of the samples

The results of purity measurements from image analysis of the gel electrophoresis experiments and the monomer content determined SEC are reported in Table 2. The purity of the samples was high with the exception of some of the samples from recombinant rice: A, B, C, H, and K. These samples were included as examples of the products available, but the DSC data was not included. The molecular weight of the samples was determined using MALDI-TOF mass spectrometry. The molecular weight data is consistent with a full length HSA molecule. HSA is translated in a precursor form with a signal and a pro-peptide of 609 amino acids. The secreted form has 585 amino acids with a theoretical molecular weight of 66,472.2 (www. Expasy.org, P02768). The molecular weight of the all samples was within the estimated uncertainty of the measurement with an average value



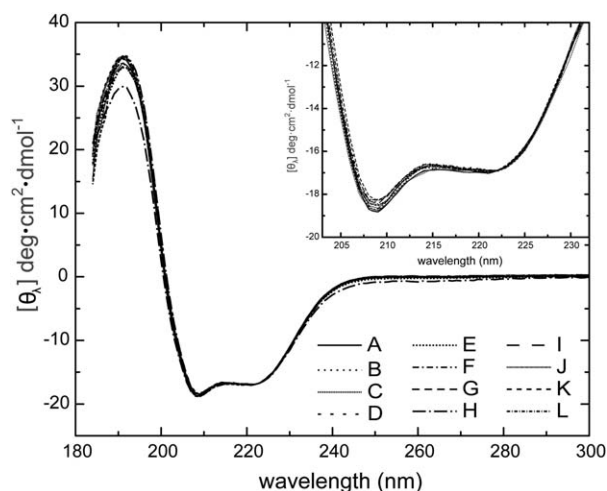


**Figure 1.** Circular dichroism spectra of 50  $\mu$ M HSA samples A through L (as is) from 184 nm to 300 nm.

Inset shows the same spectra from 200 nm to 240 nm.

66,450 Da. The molecular mass of the samples did not change after defatting, indicating that MALDI-TOF stripped the protein of non-covalently bound ligands.

The fatty acid content of the samples as received and after defatting (samples E, G, and I) was measured using a fluorescent assay with palmitic acid (hexadecanoic acid) as the fatty acid standard. The fatty acids levels of the samples are shown in Table 2.

#### Circular dichroism measurements of the samples

The CD measurements for samples A through J are shown in Figure 1. For comparison purposes, and because of slight concentration differences, the total signals were normalized to value of sample E-1 at 222 nm. The CD measurements of the albumin samples indicate that there is a very little difference in the samples that can be seen by using this method. The one exception is the G-1 sample (yeast) which has a slightly less intense peak at 191 nm. The CD measurements show that the albumin samples are primarily alpha helices, which is consistent with what is known about the albumin structure.<sup>27–29</sup> Unfortunately, the CD data does not reveal any finer structural details and cannot give information on the subtle changes to the tertiary structure of albumins that are likely the source of differences in the calorimetric data.

#### DSC measurements

Previous DSC measurement by Shrake et al. have demonstrated that the although HSA has a propensity to aggregate on denaturation, the unfolding transition itself is microscopically reversible with respect to the individual protein macromolecules.<sup>17</sup> To analyze the DSC data, we used the Origin software package from the manufacturer to model the behavior of the heat capacity curves. Baselines were subtracted from the total heat capacity curves using a cubic function to interpolate the heat capacity change in the transition region,  $\Delta C_p$  and this is the heat capacity shown in all figures. While this does not allow for the quantification of the change in heat capacity between the folded and unfolded states, it allowed for consistency of measurement of  $T_m$  and the transition enthalpy, since the samples could not be modeled with a simple set of two-state transitions. All of the samples were

**Table 3.** Melting Temperatures, Calorimetric Enthalpies, and van't Hoff Enthalpies for the Primary Transition for the Different HSA Samples

Sample	$T_{m,1}$ ( $^{\circ}$ C)	Initial Fatty Acid Level (x)	$\Delta H_{cal,1}$ ( $\text{kJ mol}^{-1}$ )	$\Delta H_{vH,1}$ ( $\text{kJ mol}^{-1}$ )	$T_{m,2}$ ( $^{\circ}$ C)
D	$65.1 \pm 0.4$	0.2	$946 \pm 98$	$492 \pm 42$	$71.6 \pm 0.9$
E-1	$67.8 \pm 0.4$	0.46	$423 \pm 44$	$287 \pm 24$	$78.2 \pm 0.8$
E-2	$62.0 \pm 0.1$	0.2	$591 \pm 60$	$326 \pm 27$	$71.1 \pm 1.3$
F	$67.9 \pm 0.5$	0.6	$777 \pm 93$	$506 \pm 42$	$76.6 \pm 1.3$
G-1	$65.6 \pm 0.1$	0.1	$810 \pm 32$	$912 \pm 4$	$68.1 \pm 0.3$
G-2	$61.9 \pm 0.1$	>0.01	$694 \pm 23$	$999 \pm 24$	$64.6 \pm 0.9$
<b>I-1</b>	<b><math>69.5 \pm 0.8</math></b>	<b>0.2</b>	<b><math>560 \pm 70</math></b>	<b><math>398 \pm 33</math></b>	<b><math>81.1 \pm 0.6</math></b>
<b>I-2</b>	<b><math>62.7 \pm 0.8</math></b>	<b>0.1</b>	<b><math>517 \pm 84</math></b>	<b><math>426 \pm 36</math></b>	<b><math>66.3 \pm 0.6</math></b>
<b>J</b>	<b><math>68.2 \pm 0.4</math></b>	<b>2.4</b>	<b><math>643 \pm 114</math></b>	<b><math>704 \pm 105</math></b>	<b><math>72.8 \pm 2.5</math></b>
L	$63.3 \pm 0.1$	1.6	$747 \pm 74$	$424 \pm 17$	$73.5 \pm 0.3$
<b>M</b>	<b><math>62.4 \pm 0.1</math></b>	<b>2.2</b>	<b><math>706 \pm 53</math></b>	<b><math>486 \pm 4</math></b>	<b><math>70.8 \pm 0.6</math></b>
<b>N</b>	<b><math>66.9 \pm 0.2</math></b>	<b>4.4</b>	<b><math>562 \pm 58</math></b>	<b><math>667 \pm 11</math></b>	<b><math>72.9 \pm 0.2</math></b>
<b>O</b>	<b><math>68.1 \pm 0.2</math></b>	<b>3.6</b>	<b><math>634 \pm 23</math></b>	<b><math>329 \pm 4</math></b>	<b><math>78.7 \pm 0.3</math></b>

Values shown are calculated from multiple runs with  $\pm 2$  S.D. Samples shown in bold are from humans.

evaluated using a non-two-state model in Origin, where the fitting parameters are  $T_m$ ,  $\Delta H_{vH}$ , and  $\Delta H_{cal}$ , which are the transition temperature, the van't Hoff enthalpy, and the calorimetric enthalpy, respectively. The unfolding was modeled using a set of two independent non-two-state transitions. Other models, including a set of 2 two-state transitions, and 2 sequential non-independent transitions were evaluated but did not have as good a fit as the non-two state model.

The first peak, at  $T_{m,1}$ , is ascribed to the unfolding of the HSA domains and the second transition, at  $T_{m,2}$ , is thought to be due to the effects of the bound fatty acids on the HSA that change binding sites on the HSA during the main unfolding transition.<sup>19</sup> This creates a slightly more stable structure than is seen during the second unfolding transition at  $T_{m,2}$ .

The measured transition temperatures and enthalpies are summarized in Table 3, and examples of excess heat capacity curves are given in Figure 2. The data shows that most samples have two distinct transitions in the curve. The lower transition has  $T_{m,1}$  values between 61.9 $^{\circ}$ C and 69.5 $^{\circ}$ C, and the upper transition has  $T_{m,2}$  values between 64.6 $^{\circ}$ C and 81.1 $^{\circ}$ C. Figure 2 shows the DSC scans of the recombinant HSA expressed in transgenic rice, transgenic yeast, and HSA from pooled human blood.

A striking observation of the unfolding curves shown in Figure 2 is the presence of the prominent peak at  $\sim 80^{\circ}$ C in samples E, O, and I. We propose that most of the differences in the samples result from structural differences, most likely due to differences in the processing steps and the amount and nature of fatty acids bound to the albumin.

As shown previously, the heat capacity measurements and melting temperatures of blood derived HSA has varied from study to study, making it difficult to assess reference values for HSA. However, Shrake et al. measured the  $T_{m,1}$  for a sample of undefatted (1.5 mol FA/mol) HSA over a range of scan rates, allowing them to extrapolate to  $T_{m,1}$  with scan rate of 0 K/h, which will approximate the transition without kinetic effects.<sup>22</sup> Using the data provided by Shrake et al. we were able to extrapolate their melting point data to the current scan rate, giving a  $T_m$  of 68 $^{\circ}$ C. Samples J and O, have values of  $T_{m,1}$  that are consistent with this value, and two of the other human HSA samples have  $T_{m,1}$  values within 1 K of this value. Furthermore, sample J has a  $\Delta H_m$  that is also consistent with the value  $\Delta H_m$  of determined by Shrake

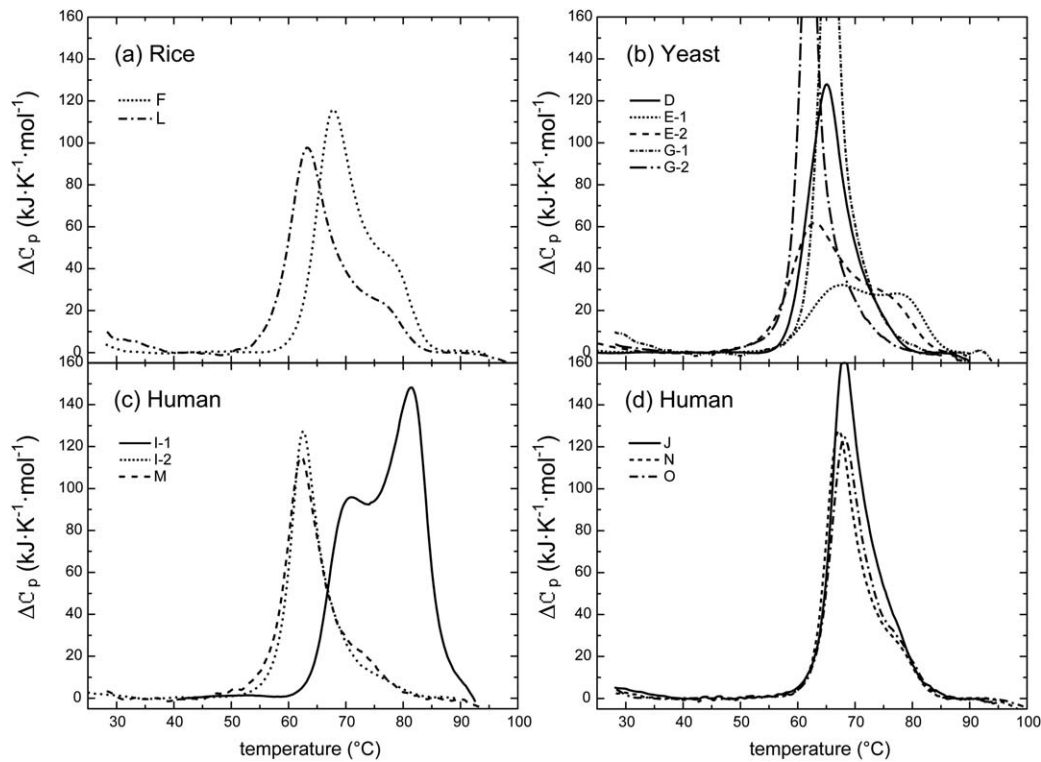


**Figure 2.** Excess heat capacity curves of the various 50  $\mu\text{M}$  HSA samples as measured on the DSC.

A: Recombinant HSA expressed in rice; (B) recombinant HSA expressed in yeast; and (C) and (D) HSA from pooled human blood. The excess heat capacity for this figure and subsequent figures is defined as the total heat capacity minus the heat capacity of the protein before and after the transition using a cubic interpolation between the two regions. Note: samples G-1 and G-2 have maximum of  $242 \text{ kJ K}^{-1} \text{ mol}^{-1}$  and  $237 \text{ kJ K}^{-1} \text{ mol}^{-1}$ , respectively.

**Table 4.** Effects of Adding 20 Mole Excess of Octanoic Acid on the Melting Temperature of HSA

	Initial Fatty Acid Level (x)	$T_{m,1}$ as is ( $^{\circ}\text{C}$ )	$T_{m,1}$ 20x c8 ( $^{\circ}\text{C}$ )	$\Delta T_{m,1}$	$\Delta H_{\text{cal}}$ ( $\text{kJ mol}^{-1}$ )
D	0.2	$65.1 \pm 0.4$	$71.0 \pm 0.1$	$5.9 \pm 0.4$	1368
E-1	0.46	$67.8 \pm 0.4$	$72.4 \pm 0.3$	$4.6 \pm 0.5$	1371
E-2	0.2	$62.0 \pm 0.1$	$72.8 \pm 0.2$	$10.8 \pm 0.2$	1385
F	0.6	$67.9 \pm 0.5$	$72.5 \pm 0.3$	$4.6 \pm 0.6$	1433
G-1	0.1	$65.6 \pm 0.1$	$70.4 \pm 0.4$	$4.8 \pm 0.4$	1373
G-2	>0.01	$61.9 \pm 0.1$	$71.3 \pm 0.6$	$9.4 \pm 0.6$	1416
<b>I-1</b>	<b>0.2</b>	<b><math>69.5 \pm 0.8</math></b>	<b><math>72.4 \pm 0.5</math></b>	<b><math>2.9 \pm 0.9</math></b>	<b>1159</b>
<b>I-2</b>	<b>0.1</b>	<b><math>62.7 \pm 0.8</math></b>	<b><math>71.7 \pm 0.1</math></b>	<b><math>9.0 \pm 0.8</math></b>	<b>1421</b>
<b>J</b>	<b>2.4</b>	<b><math>68.2 \pm 0.4</math></b>	<b><math>71.3 \pm 0.2</math></b>	<b><math>3.1 \pm 0.4</math></b>	<b>1220</b>
L	1.6	$63.3 \pm 0.1$	$71.1 \pm 0.2$	$7.8 \pm 0.2$	1201
<b>M</b>	<b>2.2</b>	<b><math>62.4 \pm 0.1</math></b>	<b><math>71.5 \pm 0.3</math></b>	<b><math>9.1 \pm 0.3</math></b>	<b>1140</b>
<b>N</b>	<b>4.4</b>	<b><math>66.9 \pm 0.2</math></b>	<b><math>72.0 \pm 0.4</math></b>	<b><math>5.1 \pm 0.4</math></b>	<b>1092</b>
<b>O</b>	<b>3.6</b>	<b><math>68.1 \pm 0.2</math></b>	<b><math>73.1 \pm 0.1</math></b>	<b><math>5.0 \pm 0.2</math></b>	<b>1386</b>

Values shown are calculated from multiple runs with  $\pm 2$  S.D. Samples shown in bold are from humans.

et al. as well.<sup>22</sup> An average value of the primary transition from pooled plasma HSA samples (I-1, J, N, and O, all with fatty acids) gives a of  $T_{m,1} = 68.2^{\circ}\text{C}$ . Shrake et al. also measured the  $T_{m,1}$  and  $\Delta H_m$  of defatted HSA as  $64.7^{\circ}\text{C}$  and  $242.9 \text{ kcal mol}^{-1}$ , ( $1016 \text{ kJ mol}^{-1}$ ) respectively.<sup>17</sup>

#### Effect of fatty acids on transition temperatures

The amount and chain length of the fatty acid added to HSA will shift the  $T_m$  higher with varying degrees of effectiveness.<sup>17</sup> The addition of octanoic (caprylic) acid will increase the transition temperature of HSA proportionally to the amount of fatty acid added to the solution, but only up to the addition of 15 mol fraction excess of the octanoic acid.<sup>15</sup> Additional octanoic acid will not serve to further enhance the stability of the HSA.<sup>17</sup> A study using CD and

gel electrophoresis to measure thermal unfolding and aggregation found that adding 1 mM octanoic acid ( $\sim 125$  molar excess) to BSA (Cohn Fraction V) stabilized the protein against a heat step ( $60^{\circ}\text{C}$  for 30 min) by preventing aggregation and increased the melting temperature by  $3^{\circ}\text{C}$ .<sup>30</sup>

We have added a 20 mol excess of octanoic acid (sodium salt) to the samples shown in Table 4 to determine the shift in the  $T_{m,1}$ . The  $T_{m,1}$  for each of the samples was increased due to the addition of the fatty acid, however the magnitude of the change was not the same for all of the samples. Rather, the change in melting temperature was inversely proportional to the initial  $T_{m,1}$ , and the resulting transition temperature for all the samples was consistent at  $71.8^{\circ}\text{C}$  (S.D. 0.8) on the additional excess amounts of octanoic acid. The resulting excess heat capacity curves can be seen in Figure 3.

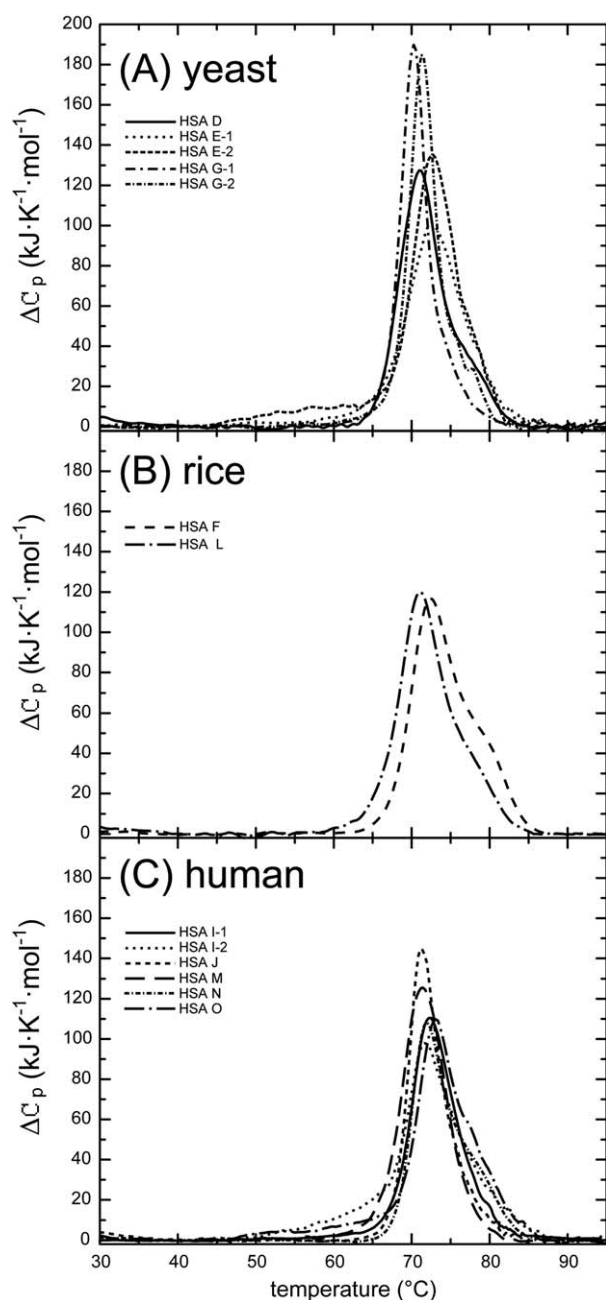


**Figure 3.** Effect of adding 20 mole excess of octanoic acid on the melting temperature of 50  $\mu\text{M}$  HSA.

Samples are as shown in legend. Data from the curves are shown in Table 4.

While there is still some variation in the curves for each of the HSA samples, the curves are much more consistent in shape and peak height than the samples without the octanoic acid. As with the melting temperature, the total enthalpy of transition did not increase the same magnitude with the same molar addition of octanoic acid, but  $\Delta H_{\text{cal}}$  similar for each of the samples, with an average value of 1300 (S.D. 122  $\text{kJ mol}^{-1}$ ). Splitting the results by type,  $\Delta H_{\text{cal}}$  for the recombinant samples is 1,360 (S.D. 75  $\text{kJ mol}^{-1}$ ) and for the pooled serum samples  $\Delta H_{\text{cal}}$  is 1,240 (S.D. 124  $\text{kJ mol}^{-1}$ ).

#### Effect of pasteurization on the unfolding measurements

Pasteurization of HSA from pooled plasma is an important step to minimize the risk of blood borne pathogens and

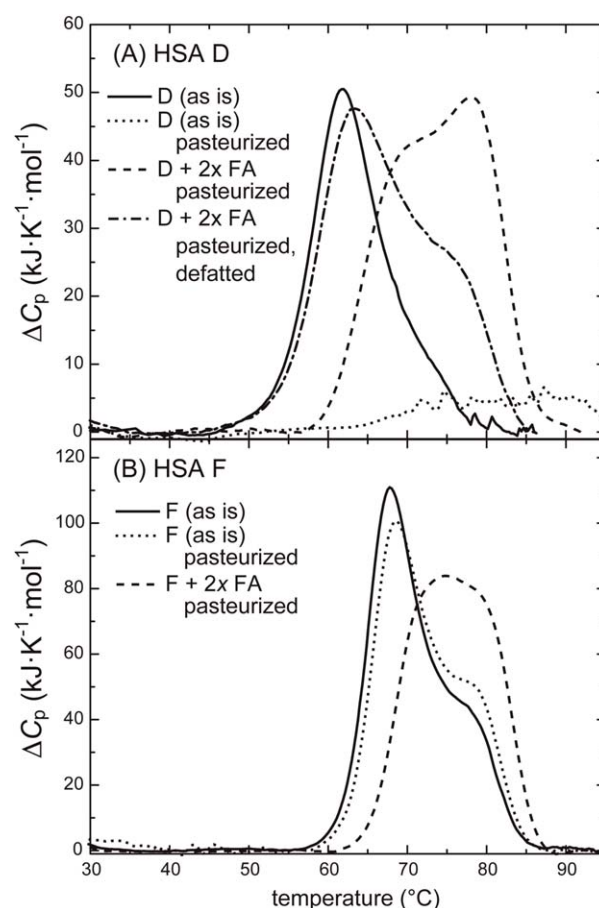


**Figure 4.** Effect of a pasteurization step (60°C for 12 h) on HSA samples.

A: Solid line yeast sample D (as is, defatted by supplier); Dotted line sample D pasteurized; Dashed line sample D pasteurized in the presence of 2 moles of *cis* 9-octadecenoic acid; Dashed and dotted line sample D pasteurized in the presence of 2 mol of *cis* 9-octadecenoic acid and then defatted. B: Solid line sample F (as is from supplier, containing 0.6 mol fraction fatty acid); Dotted line sample F (as is) pasteurized; Dashed line sample F pasteurized in the presence of 2 mole fraction of *cis* 9-octadecenoic acid. Samples run are 50  $\mu\text{M}$ .

improve the purification process by precipitating contaminants. We examined this step to determine whether pasteurization results in the increased stability seen in some of the samples. Several samples of HSA were pasteurized in the presence and absence of fatty acids.

The excess heat capacity curves of sample D (yeast) is shown in Figure 4. Sample D has an initial low content of fatty acid (defatted by supplier, 0.2 mol fraction remaining). When this sample is pasteurized the tertiary structure is destroyed, as shown by the absence of any unfolding transitions (Figure 4). Pasteurization of sample D in the presence of 2 mol of *cis* 9-octadecenoic acid stabilized the protein, resulting in enhanced stability. The calculated melting temperatures  $T_{m1}$  and  $T_{m2}$  for the two transitions of the pasteurized sample are 71.1°C and 77.9°C, respectively. When sample D was pasteurized in the presence of 2 mol of *cis* 9-octadecenoic acid and then defatted with the low pH method, the transition temperature was shifted back to almost to the original value (Figure 4). Sample F (rice), with 0.6 mol fraction of fatty acids (as is), was pasteurized as supplied and also with 2 mol fractions of *cis* 9-octadecenoic acid added to the sample. Sample F had sufficient fatty acids as supplied

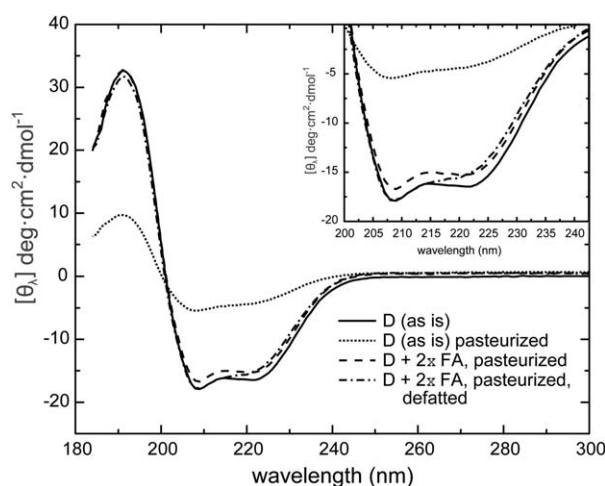


**Figure 5.** Circular dichroism spectra of yeast sample D (as is, defatted by supplier). Samples: solid line (as is); dotted line (as is and pasteurized); dashed line (pasteurized in the presence of 2 mol of *cis* 9-octadecenoic acid; and dashed and dotted line (pasteurized in the presence of 2 mol of *cis* 9-octadecenoic acid and then defatted). Inset: magnified view of CD spectra from 202 nm to 232 nm.

to prevent the loss of structure during pasteurization, and in the presence of 2 mol of *cis* 9-octadecenoic acid, the curve was shifted to the more stable form during pasteurization (Figure 4). A sample of F containing 2 mol *cis* 9-octadecenoic acid added was pasteurized at 60°C for 24 h and gave the same results as the sample pasteurized for 12 h (data not shown).

Thus, the presence of fatty acids during the pasteurization process not only stabilizes the albumin into a stable configuration, but the original structure can be restored on the removal of the fatty acids. This is likely due to the physical changes in the protein that occur during the defatting process.<sup>28,31</sup> When adjusting the pH below 4.0 to begin the defatting, the lower pH drives the albumin to open up its structure about domain 2, similar to the operation of a hinge.<sup>23</sup> Removal of the fatty acids and restoration of the pH to near neutral, the protein folds back to lower stability conformation.

CD measurements on the pasteurized HSA samples are consistent with the changes in structure due to pasteurization and defatting. Figure 5 shows the CD spectra for the unpasteurized sample D (yeast), pasteurized sample D, pasteurized D with 2 mol excess of *cis* 9-octadecenoic acid, and sample D pasteurized with 2 mol of *cis* 9-octadecenoic acid and then defatted. The most striking difference in the CD spectra comes from the pasteurized defatted HSA, where there is a distinct shift in the CD peak near 210 nm and a change in shape of the peak as well. While this sample was shown to be in the unfolded state using DSC, the CD spectrum shows that the HSA does retain much of the  $\alpha$ -helical structure on unfolding. The proteins pasteurized with fatty acids have CD spectra with the same overall shape as the unpasteurized sample, indicating there is no significant change to the  $\alpha$ -helical structure even though the tertiary structure, as evidenced by the DSC results, has been modified.

#### Effect of the low pH defatting process

To further explore the structural changes of albumin by the defatting process, samples E-2 (yeast), G-2 (yeast), and

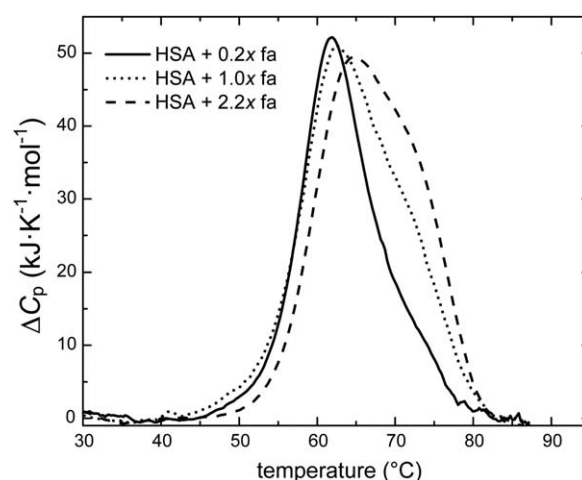


**Figure 6.** Excess heat capacity curves of sample E-2 (yeast defatted, 0.2 mol fraction fatty acids remaining). Samples: solid line (as is); dotted line sample E-2 with 1 mol *cis* 9-octadecenoic acid added; and dashed line sample E-2 with 2.2 mol *cis* 9-octadecenoic acid added. Samples run are 50  $\mu$ M.

I-2 (human) were obtained from the original stock materials by defatting at low pH, consequently opening and closing the domains of the albumin. As can be seen in Figure 2 and Table 3, the defatting process decreased  $T_{m1}$  by 5.8°C, 3.7°C, and 6.8°C for samples E, G, and I, respectively. It should be noted that since initially sample G did not contain a significant amount of fatty acids (mole fraction = 0.12) as provided by the supplier, the change in  $T_{m1}$  is due primarily to structural changes and not to the fatty acid content. The defatted samples had a consistent  $T_{m1}$  (average of 62.2°C).

We added 1 or 2.2 mole fractions of *cis* 9-octadecenoic acid per mole of HSA to E-2, a defatted yeast sample (Figure 6). There is an increase in the  $T_{m2}$ , seen as a shoulder that is proportional to the increase of the amount of fatty acid in the sample. There is also an increase in  $T_{m1}$  as the amount of *cis* 9-octadecenoic acid is increased on the albumin. The addition of 2.2 mole fractions *cis* 9-octadecenoic acid increased  $T_{m1}$  by 2.7°C. Although this is consistent with previous observation, the shift in  $T_{m1}$  is less than that of the original change of 5.8°C on defatting, and the amount of fatty acid removed was significantly less than the quantity of *cis* 9-octadecenoic acid added back to the albumin. Thus, the decrease in  $T_{m1}$  is not solely due to the removal of the fatty acids alone, but may also be indicative of a structural change as well.

## Conclusions

The size and shape of the DSC peaks of the commercial products are quite variable as demonstrated in Figure 2. Part of the size of the secondary peak may be attributed to the mole fraction of fatty acids present and also to the length and saturation of the fatty acids. Perhaps just as important is the location of where the fatty acids bind on the albumin molecule. There are seven fatty acid binding sites identified on HSA and presumably two high affinity binding sites. This correlates well with the current model that HSA in the blood carries about two long-chain fatty acid molecules.<sup>32</sup> Thus, there are potentially a number of possible distributions of fatty acids on the protein that can influence the thermal stability.



We have shown that there is a wide variation in melting temperature and enthalpy of transitions between different sources of HSA, even between different lots from the same manufacturer. We have demonstrated differences in  $T_{m1}$  may arise from the effects of added fatty acids and heat pasteurization. A simple model of the different structural states and resulting ranges of melting temperatures of HSA would be:



$$T_m \sim 62^\circ\text{C} \sim 64\text{--}72^\circ\text{C} \sim 75\text{--}80^\circ\text{C}$$

The initial binding of fatty acids to HSA increases the stability of the HSA fatty acid complex by a range of values depending upon the amount and nature of the fatty acids. Prolonged incubation at  $60^\circ\text{C}$  (pasteurization) results in a further stabilization to a  $T_m$  of approximately  $75\text{--}80^\circ\text{C}$ . We have also shown that the process is reversible by the low pH defatting process. When octanoic acid was added to the HSA samples prior to DSC, the data from the measurements were consistent indicating that the resulting structures are the same. The prolonged incubation of the HSA(FA) complex at  $60^\circ\text{C}$  results in a protein structure with high stability. These results show the importance of the bioprocessing steps on the stability of HSA products from both human donors and recombinant sources.

### Literature Cited

- Peters T. *All About Albumin Biochemistry, Genetics, and Medical Applications*. San Diego, CA: Academic Press; 1996.
- Sleep D, Cameron J, Evans LR. Albumin as a versatile platform for drug half-life extension. *Biochim Biophys Acta*. 2013;1830:5526–5534.
- Perkins M. Recombinant albumin facilitates formulation design of stable drug products. *BioPharm Int*. 2012;25:40–44.
- Chen Z, He Y, Shi B, Yang D. Human serum albumin from recombinant DNA technology: challenges and strategies. *Biochim Biophys Acta*. 2013;1830:5515–5525.
- He Y, Ning TT, Xie TT, Qiu QC, Zhang LP, Sun YF, Jiang DM, Fu K, Yin F, Zhang WJ, Shen L, Wang H, Li JJ, Lin QS, Sun YX, Li HZ, Zhu YG, Yang DC. Large-scale production of functional human serum albumin from transgenic rice seeds. *Proc Natl Acad Sci USA*. 2011;108:19078–19083.
- Watanabe H, Yamasaki K, Kragh-Hansen U, Tanase S, Harada K, Suenaga A, Otagiri M. In vitro and in vivo properties of recombinant human serum albumin from *Pichia pastoris* purified by a method of short processing time. *Pharm Res*. 2001;18:1775–1781.
- Sleep D, Belfield GP, Goodey AR. The secretion of human serum albumin from the yeast *Saccharomyces cerevisiae* using five different leader sequences. *Biotechnology*. 1990;8:42–46.
- Zhu J, Wooh JW, Hou JJ, Hughes BS, Gray PP, Munro TP. Recombinant human albumin supports single cell cloning of CHO cells in chemically defined media. *Biotechnol Prog*. 2012;28:887–891.
- Sagar SL, Beitle RR, Atai MM, Domach MM. Metal-based affinity separation of alpha- and gamma-chymotrypsin and thermal stability analysis of isolates. *Bioseparation*. 1992–1993;3:291–296.
- Choi JK, Ho J, Curry S, Qin DH, Bittman R, Hamilton JA. Interactions of very long-chain saturated fatty acids with serum albumin. *J Lipid Res*. 2002;43:1000–1010.
- Simard JR, Zunszain PA, Hamilton JA, Curry S. Location of high and low affinity fatty acid binding sites on human serum albumin revealed by NMR drug-competition analysis. *J Mol Biol*. 2006;361:336–351.
- Ascenzi P, Fasano M. Allosterism in monomeric protein: the case of human serum albumin. *Biophys Chem*. 2010;148:16–22.
- Celej MS, Dassie SA, onzalez, M.; Bianconi ML, Fidelio GD. Differential scanning Calorimetry as a tool to estimate binding parameters in multiligand binding proteins. *Anal Biochem*. 2006;350:227–284.
- Michnik A, Michalik K, Kluczevska A, Drzazga Z. Comparative DCS study of human and bovine serum albumin. *J Therm Anal Calorim*. 2006;84:113–117.
- Pico GA. Thermodynamic features of the thermal unfolding of human serum albumin. *Int J Biol Macromol*. 1997;20:63–73.
- Rezaei-Tavirani M, Moghaddamnia SH, Ranjbar B, Amani M, Marashi, S.-A., conformational study of human serum albumin in pre-denaturation temperatures by differential scanning calorimetry, circular dichroism and UV spectroscopy. *J Biochem Mol Biol*. 2006;39:530–536.
- Shrake A, Frazier D, Schwarz FP. Thermal stailization of human albumin by medium- and short-chain n-alkyl fatty acid anions. *Biopolymers*. 2006;81:235–248.
- Farruggia B, Rodriguez F, Rigatuso R, Fidelio G, Pico G. The participation of human serum albumin domains in chemical and thermal unfolding. *J Protein Chem*. 2001;20:81–89.
- Michnik A. Thermal stability of bovine serum albumin DSC study. *J Therm Anal Calorim*. 2003;71:509–519.
- Yamasaki M, Yano H, Aoki K. Differential scanning calorimetric studies on bovine serum albumin. I. Effects of pH and ionic strength. *Int J Biol Macromol*. 1989;12:263–268.
- Garidel P, Hoffmann C, Blume A. A thermodynamic analysis of the binding interaction between polysorbate 20 and 80 with human serum albumins and immunoglobulins: a contribution to understand colloidal protein stabilisation. *Biophys Chem*. 2009;143:70–78.
- Shrake A, Finlayson JS, Ross PD. Thermal stability of human albumin measured by differential scanning calorimetry. *Vox Sang*. 1984;47:7–18.
- Kragh-Hansen U. A micromethod for delipidation of aqueous proteins. *Anal Biochem*. 1993;210:318–327.
- Tanaka K, Shigueoka EM, Sawatani E, Dias GA, Arashiro F, Campos TCXB, Nakao HC. Purification of human albumin by the combination of the method of Cohn with liquid chromatography. *Braz J Med Biol Res*. 1998;31:1383–1388.
- Koorevaar G, Stekelenburg V. Mammalian acetocetate decarboxylase activity: its distribution in subfraction of human albumin and occurrence in various tissues of the rat. *Clin Chim Acta*. 1976;71:173–183.
- Michnik A, Michalik K, Drzazga Z. Stability of bovine serum albumin at different pH. *J Therm Anal Calorim*. 2006;80:399–406.
- Kragh-Hansen U, Chuang VTG, Otagiri M. Practical aspects of the ligand-binding and enzymatic properties of human serum albumin. *Biol Pharm Bull*. 2002;25:695–704.
- Curry S, Mandelkow H, Brick P, Franks N. Crystal structure of human serum albumin complexed with fatty acid reveals an asymmetric distribution of binding sites. *Nat Struct Biol*. 1998;5:827–835.
- Sugio S, Kashima A, Mochizuki S, Noda MKK. Crystal structure of human serum albumin at 2.5 Å resolution. *Protein Eng*. 1999;12:439–446.
- Arakawa T, Kita Y. Stabilizing effects of caprylate and acetyltryptophanate on heat-induced aggregation of bovine serum albumin. *Biochim Biophys Acta*. 2000;1479:32–36.
- Fang YN, Tong GC, Means GE. Structural changes accompanying human serum albumin's binding of fatty acids are concerted. *Biochim Biophys Acta*. 2006;1764:285–291.
- Chuang VTG, Otagiri M. How do fatty acids cause allosteric binding of drugs to human serum albumin? *Pharm Res*. 2002;19:1458–1464.

Manuscript received Aug. 6, 2014, and revision received Sept. 11, 2014.